Check for updates

ChemPhysChem

Chemistry Europe
European Chemical Societies Publishing

Accepted Article

Title: Indirectly Detected DNP-Enhanced 17O NMR Spectroscopy: Observation of Non-Protonated Near-Surface Oxygen at Naturally Abundant Silica and Silica-Alumina

Authors: Takeshi Kobayashi and Marek Pruski

This manuscript has been accepted after peer review and appears as an Accepted Article online prior to editing, proofing, and formal publication of the final Version of Record (VoR). This work is currently citable by using the Digital Object Identifier (DOI) given below. The VoR will be published online in Early View as soon as possible and may be different to this Accepted Article as a result of editing. Readers should obtain the VoR from the journal website shown below when it is published to ensure accuracy of information. The authors are responsible for the content of this Accepted Article.

To be cited as: *ChemPhysChem* 10.1002/cphc.202100290

Link to VoR: https://doi.org/10.1002/cphc.202100290

WILEY-VCH

WILEY-VCH

COMMUNICATION

Indirectly Detected DNP-Enhanced ^{17}O NMR Spectroscopy: Observation of Non-Protonated Near-Surface Oxygen at Naturally Abundant Silica and Silica-Alumina

Takeshi Kobayashi*[a] and Marek Pruski[a]

[a] Dr. T. Kobayashi, Prof. M. Pruski
U.S. DOE Ames Laboratory
Iowa State University
Ames, Iowa 50011-3020, United States
E-mail: takeshi@iastate.edu

Supporting information for this article is given via a link at the end of the document.

Abstract: Recent studies have shown that dynamic nuclear polarization (DNP) can be used to detect ^{17}O solid-state NMR spectra of naturally abundant samples within a reasonable experimental time. Observations using indirect DNP, which relies on ^{1}H mediation in transferring electron hyperpolarization to ^{17}O, are currently limited mostly to hydroxyls. Direct DNP schemes can hyperpolarize non-protonated oxygen near the radicals; however, they generally offer much lower signal enhancements. In this study, we demonstrate the detection of signals from non-protonated ^{17}O in materials containing silicon. The sensitivity boost that made the experiment possible originates from three sources: indirect DNP excitation of ^{29}Si via protons, indirect detection of ^{17}O through ^{29}Si nuclei using two-dimensional $^{29}Si\{^{17}O\}$ *D*-HMQC, and Carr-Purcell-Meiboom-Gill refocusing of ^{29}Si magnetization during acquisition. This ^{29}Si-detected scheme enabled, for the first time, 2D ^{17}O-^{29}Si heteronuclear correlation spectroscopy in mesoporous silica and silica-alumina surfaces at natural abundance. In contrast to the silanols showing motion-averaged ^{17}O signals, the framework oxygens exhibit unperturbed powder patterns as unambiguous fingerprints of surface sites. Along with hydroxyl oxygens, detection of these moieties will help in gaining more atomistic-scale insights into surface chemistry.

Oxygen is a ubiquitous element in biochemistry and materials science, yet one that challenges solid-state (SS)NMR spectroscopy, mainly due to the very low natural abundance of its only NMR-active isotope, ^{17}O (0.038 %). The lack of sensitivity is further exacerbated in studies of diluted species on surfaces of materials. The ^{17}O nuclide is also quadrupolar (I = 5/2), and while its quadrupolar moment is moderate (Q = -25.58 mb), the resulting line broadening complicates spectral analysis. Thus far, ^{17}O SSNMR experiments have strongly depended on ^{17}O isotopic enrichment, which limited their use due to synthetic difficulties and high cost.

Recently, dynamic nuclear polarization (DNP) NMR has opened the way for detecting signals of unreceptive nuclides which suffer from low gyromagnetic ratios, low natural abundance, dilution, line broadening or any combination of these challenges.[1-15] As a matter of course, researchers have applied this emerging technique to the ^{17}O nuclide, and demonstrated that ^{17}O SSNMR spectra could be acquired at natural abundance from nanoparticles[4, 9, 12-13, 15-17] and even from surfaces.[9, 18-21] In the majority of studies, however, the hyperpolarization of ^{17}O nuclei has been achieved via protons using the route $e^- \rightarrow {}^{1}H \rightarrow ({}^{1}H–{}^{1}H$ spin diffusion$) \rightarrow {}^{17}O \rightarrow$ detection. This protocol, termed indirect DNP, relies on propagation of magnetization throughout the sample via $^{1}H–^{1}H$ spin diffusion, before the final $^{1}H \rightarrow {}^{17}O$ polarization transfer. Although the indirect DNP scheme is generally most sensitive and thus predominantly used, its applications are limited by the short-range nature of the $^{1}H \rightarrow {}^{17}O$ transfer. Indeed, the natural abundance ^{17}O DNP NMR has been mostly restricted to protonated oxygens, i.e. hydroxyls,[4, 9, 12, 18-19] with one exception of a recent report on the use of *D*-RINEPT.[21] The use of advanced radical molecules[20, 22-24] or suitable metal ions[13, 15] has enabled a direct, $e^- \rightarrow {}^{17}O$ DNP route; however, the absence of ^{17}O-^{17}O spin diffusion in naturally abundant samples keeps most spins unpolarized.

In this study, we demonstrate a DNP approach that efficiently detects ^{17}O signals from non-enriched and non-protonated oxygens through other nuclei, in this case ^{29}Si, using a multi-step scheme $e^- \rightarrow {}^{1}H \rightarrow {}^{29}Si \rightarrow {}^{17}O \rightarrow {}^{29}Si \rightarrow CPMG_{acq}$ (Figure 1). (1) In the first step, the electrons' hyperpolarization is transferred to ^{29}Si via the abovementioned indirect DNP route $e^- \rightarrow {}^{1}H \rightarrow {}^{29}Si$, using cross-polarization (CP) for the $^{1}H \rightarrow {}^{29}Si$ transfer. (2) The second step employs the two-dimensional (2D) $^{29}Si\{^{17}O\}$ dipolar heteronuclear multiple quantum correlation (*D*-HMQC) spectroscopy. *D*-HMQC has recently become the method of choice for the studies of spatial proximity between heteronuclei in solids,[25-26] because of the inherent low efficiency in polarization transfer from ^{1}H to a quadrupolar nuclei such as ^{17}O by cross-polarization. Here, we use the symmetry-based SR4 sequence[27] for $^{29}Si–^{17}O$ heteronuclear recoupling, because it is easy to optimize, tolerant of resonance offsets, and has low RF requirements that can be easily met by our DNP MAS probe in its ^{1}H-^{29}Si-^{17}O configuration. Note that alternative recoupling schemes, such as SFAM, could be considered; however, T_2' relaxation losses are insignificant in our experiment.[28] In the proposed scheme, HMQC detects the ^{17}O signal through the more sensitive ^{29}Si nuclei; note that this detection method is incidentally also termed 'indirect'.[29-30] In contrast to the typically used indirect detection via ^{1}H, however, it can be used here without fast magic-

This article is protected by copyright. All rights reserved.

Accepted Manuscript

angle spinning (MAS).[14, 29-30] Importantly, the slow T_2' relaxation of the ^{29}Si nuclide enables the implementation of step (3), namely the use of Carr-Purcell-Meiboom-Gill (CPMG) acquisition to further boost the sensitivity.[31] The CPMG interval was set to 1.2 ms, so the separation of spikelets is equivalent to the difference in chemical shift between silicon sites Q^2 and Q^3, and Q^3 and Q^4 ((≡SiO)$_2$**Si**(OH)$_2$, (≡SiO)$_3$**Si**(OH), and (≡SiO)$_4$**Si**, respectively).

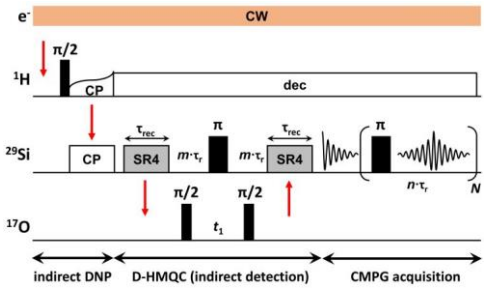

Figure 1. Pulse sequence to acquire non-protonated ^{17}O NMR spectra at natural abundance with DNP.

We first used the previously studied sample of 20% ^{17}O-enriched silica gel[9, 18] to (i) demonstrate the ability of ^{29}Si{^{17}O} *D*-HMQC to detect non-protonated oxygen sites and (ii) test the efficacy of ^{29}Si refocusing by CPMG. Figures 2a and 2b compare the DNP spectra obtained with direct polarization (DP)MAS and ^{17}O{^{1}H} PRESTO, which was effectively enhanced by CPMG due to favorable T_2' value for ^{17}O in this sample. The DPMAS spectrum represents the MAS-scaled central transition of siloxane oxygens in silica, which is additionally broadened by the distribution of local structural parameters, namely the Si-O-Si tetrahedral bond angles and Si-O distances.[32-33] Note that the direct ^{17}O DNP enhancement was very low in this sample (~1.3, see Figure S2 in the Supporting Information). Thus, most of the ^{17}O nuclei were excited by the direct (non-DNP) process, resulting in uniform polarization of silica gel and the observed predominance of siloxane oxygens in the spectra. As expected, the PRESTO MAS spectrum shows the signal almost exclusively from surface silanol oxygens, and agrees with those observed previously in mesoporous silicas SBA-15 and MCM-41.[9, 18]

The 2D ^{29}Si{^{17}O} *D*-HMQC-CPMG spectrum (Figure 2c) showed strong ^{17}O–^{29}Si correlation signals. Interestingly, the ^{17}O skyline projection of this spectrum bears closer resemblance to the DPMAS spectrum than the PRESTO MAS (see the top of Figure 3c), suggesting that the technique effectively illuminates the non-protonated siloxane oxygen sites at or near the surface. Note that the preponderance of siloxane oxygen in the HMQC spectrum is not surprising. Under the CP conditions used in our study (^{1}H → ^{29}Si CP time = 8 ms), the contribution of Q^4 sites was ~35%. Considering the fact that a Q^3 site bonds to three siloxane oxygens and only one hydroxyl oxygen, about 84% of surface oxygens detected in the HMQC spectrum is involved in Si-O-Si linkages. One notable difference between the two spectra is the emphasized singularity at -30 ppm. The ^{17}O DPMAS signals from the entire particle is given as the sum of subspectra with various η_Q values which reflect the distribution of Si–O–Si angle in the silica particles. [31, 32] In contrast, the DNP-enhanced D-HMQC measurement comprises the signals from ^{17}O near the surface. The different ^{17}O lineshapes obtained using DPMAS and D-HMQC indicate that the Si–O–Si angles near the surface are wider than those in the bulk. According to the analysis reported in ref. 32 such change suggests that the surface siloxanes exhibit wider Si-O-Si angles that those in the bulk. The signal from silanol oxygens appears to be too weak to be clearly discerned. Note that we did not detect any significant differences between ^{17}O line shapes associated with spikelets at δ ^{29}Si = -90 ppm, -100 ppm and -110 ppm. Figure 2d shows the ^{17}O–^{29}Si correlation spectrum obtained using the same experimental conditions except for the CPMG acquisition. As can be seen in their ^{17}O projections, the CPMG acquisition of ^{29}Si signal offered a roughly 10-fold signal enhancement.

We applied this method to naturally abundant MCM-41 silica and silica-alumina (SIRAL® 40/HPV, with Al:Si ratio of 3:2, see the Supporting Information), and successfully obtained the 2D ^{17}O–^{29}Si correlation spectra after 60-70 h of acquisition for each (Figure 3b and 3e, respectively). In MCM-41 silica, the ^{17}O projection of the correlation spectrum showed a signal similar to that of the ^{17}O enriched silica gel, with a center of gravity at a lower field than that of the ^{17}O signal obtained by PRESTO MAS (Figure 3a), which again corroborates the detection of non-protonated oxygens near the surface.

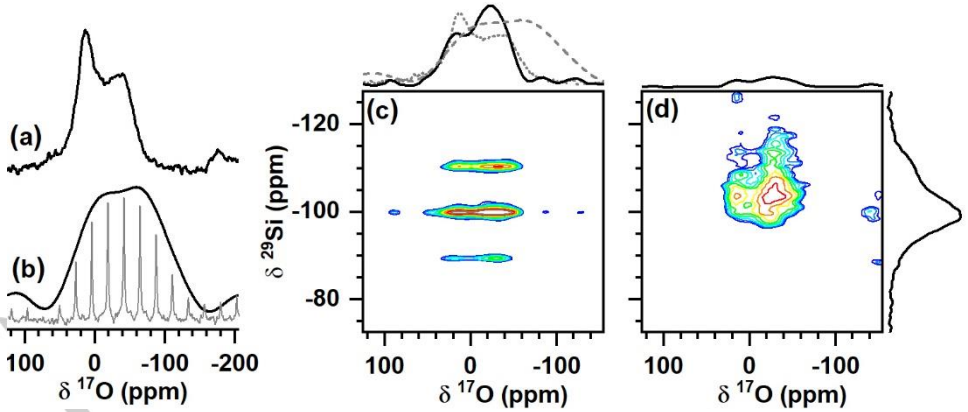

Figure 2. DNP-enhanced MAS NMR spectra of 20% ^{17}O-enriched silica acquired using 1D ^{17}O DPMAS (a), 1D ^{17}O{^{1}H} PRESTO-CPMG (b), and 2D ^{29}Si{^{17}O} *D*-HMQC with (c) and without CPMG acquisition (d). The acquisition times were 1 min (a), 7 min (b), and 1.8 h (c, d). In (b), both the spikelet (grey) and the reconstructed spectra (black) are shown. For direct comparison, the 1D ^{17}O DPMAS (dotted) and the 1D ^{17}O{^{1}H} PRESTO-CPMG (dashed) spectra are superimposed onto the ^{17}O skyline projection of the 2D *D*-HMQC spectrum (solid) in (c). The ^{17}O skyline projections in (solid lines in c, d) show the absolute intensity, demonstrating the effect of CPMG acquisition. The silica sample was impregnated with a 16 mM solution of TEKPol[34] in non-hydrogen bonding solvent (1,1,2,2-tetrachloroethane) and spun at 10 kHz at a temperature of 100~105 K. 60 echoes and 160 echoes were accumulated for the PRESTO-CPMG (b) and *D*-HMQC-CPMG (c) experiments, respectively. Note that in c and d, the direct (^{29}Si) and the indirect (^{17}O) axes are transposed for better readability of the ^{17}O projected spectra.

This article is protected by copyright. All rights reserved.

Accepted Manuscript

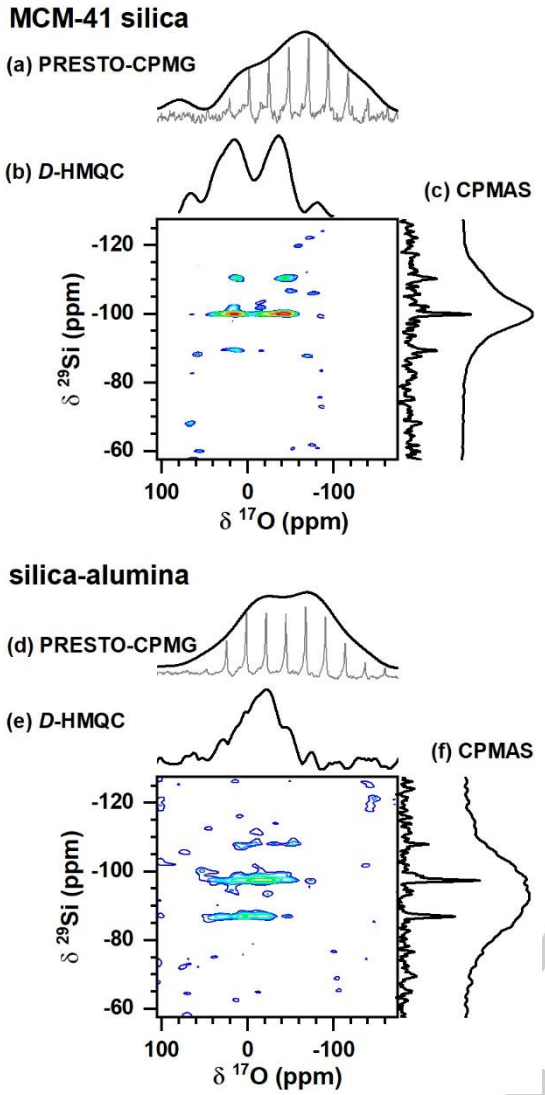

Figure 3. ^{17}O SSNMR spectra of natural abundance MCM-41 silica (a-c) and silica-alumina (d-f) acquired using the DNP-enhanced 1D $^{17}O\{^1H\}$ PRESTO-CPMG (a, d), 2D $^{29}Si\{^{17}O\}$ *D*-HMQC-CPMG (b, e), and $^{29}Si\{^1H\}$ CPMAS (c, f).. The acquisition times were 70 h (b) and 60 h (e). The enhancement factor in the $^{29}Si\{^1H\}$ CPMAS signal of MCM-41 was ~90; for silica-alumina the signal without DNP was undetectable, suggesting that the enhancement was at least 200 (see Fig. S2). For easier analysis of 2D spectra, the chemical shifts of indirectly detected nuclei (^{17}O) are shown on the horizontal axis.

The same set of experiments was performed on the silica-alumina sample. The PRESTO-derived ^{17}O spectrum (Figure 3d) was slightly broader than in Figure 3a. The ^{17}O projection of the 2D spectrum shows a featureless ^{17}O signal (Figure 3e), and again, the center of gravity of the ^{17}O signal is at a lower field of than that of the PRESTO MAS signal. The $^{29}Si\{^1H\}$ CPMAS signal of silica-alumina appeared at a lower field (centered at -90 ppm, Figure 3f) than that of MCM-41 silica (centered at -100 ppm, Figure 3c), and was assignable to $Si(–OAl)_2(–OSi)(–OH)$ (hereafter referred to as Si(2Al, Si, OH)), Si(Al, Si, 2OH), Si(3Al, Si) and Si(2Si, 2OH) species which are all expected at around -90 ppm.[35-36]

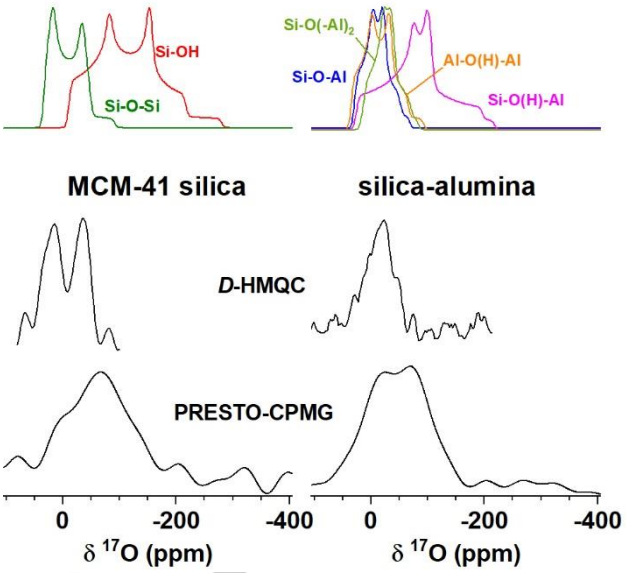

Figure 4. Simulated and experimentally obtained ^{17}O NMR spectra. The spectra of Si–O–Si, Si–OH, Si–O–Al, and $Si–O(–Al)_2$ were simulated on the basis of DFT computed NMR parameters, while that of Al–O(H)–Al was reproduced using the experimentally obtained parameters reported in Ref. 39 and 40, respectively. 500 Hz of Gaussian line broadening was applied to the simulated lines.

Table 1. DFT Computed[a] and Experimentally Obtained ^{17}O NMR Parameters

Sites	δ_{iso} (ppm)	$\lvert C_Q \rvert$ (MHz)	η_Q	source
Si–O–Si	40 (3)	5.3 (0.1)	0.22 (0.05)	this work (DFT)[b]
Si–O–Si	40[c]	5.2 (0.7)	0.2 (0.2)	ref. 37 (exp)
Si–OH	2 (1)	7.9 (0.3)	0.65 (0.05)	this work (DFT)[b]
Si–OH	-3	7.3	0.46	ref. 38 (DFT)
Si–O–Al	29 (14)	4.3 (0.7)	0.62 (0.24)	this work (DFT)
$Si–O–(Al)_2$	35 (10)	4.3 (0.6)	0.76 (0.16)	this work (DFT)
Al–O(H)–Al	40	5.0	0.5	ref. 39 (exp)
Si–O(H)–Al	28	6.6	0.8	ref. 40 (exp)

[a] Averaged value (standard deviation). [b] The DFT computed parameters for the silica slab model, which is curved from cristobalite, followed by termination of dangling bonds with hydroxyls and structural relaxation, are in good agreement with those for amorphous silicas. [c] δ_{iso} is estimated from the figure within the reference.

To make more definitive assignments, density functional theory (DFT) calculations were performed on silica and silica-alumina models (see Supporting Information for details). The computed ^{17}O NMR parameters along with the previously reported experimental values[37-40] are listed in Table 1; the corresponding spectra are drawn in Figure 4. For MCM-41, the ^{29}Si-detected ^{17}O spectrum is in good agreement with the ^{17}O spectrum simulated for Si–O–Si, whereas the PRESTO ^{17}O spectrum, which must represent mostly silanol groups, is much narrower than the corresponding simulated line for silanols. The silanol group is dynamic[38, 41] even under the DNP conditions (the presence of frozen solvent at ~100 K),[9] and the ^{17}O line width is reduced by the partial averaging of the ^{17}O electric field gradient. It has also

Accepted Manuscript

This article is protected by copyright. All rights reserved.

been reported that the elongated O–H bond length due to hydrogen bonding results in smaller C_Q values.[42] The ^{29}Si{^{17}O} *D*-HMQC spectrum of silica-alumina (Figure 3e) is considerably different from that of MCM-41. Notably, the Si–O–Si links are not present in detectable quantity. Instead, the ^{17}O projection agrees with the simulated spectra for Si–O–Al and Si–O(–Al)$_2$ links. These observations suggest that the Si and Al atoms are well intermixed, at least at or near the materials' surface, as would be expected in accordance with the Löwenstein's rule. The signal from Al–O(H)–Si link was not detected, which is consistent with the fact that that the Brønsted acid sites are rare in this material.[19] Note that another possible structure, Al–O(H)–Al, would not be observable in the ^{29}Si-detected ^{17}O spectrum. Consequently, the PRESTO MAS spectrum is attributable primarily to aluminols [19].

In summary, we demonstrated the indirect detection of ^{17}O NMR via ^{29}Si, using DNP-enhanced ^{29}Si{^{1}H} CPMAS followed by 2D ^{29}Si{^{17}O} *D*-HMQC-CPMG. By utilizing the third nucleus, ^{29}Si, this approach takes advantage of the high sensitivity of ^{1}H-mediated DNP without limiting its applications to protonated oxygen. Remarkably, the combined use of DNP, HMQC and CPMG refocusing allowed to detect ^{17}O signals from non-protonated oxygen in naturally abundant MCM-41 silica and silica-alumina. In addition, ^{17}O signals from the framework oxygens are not motion-averaged, and offer valuable structural information that cannot be obtained through mobile hydroxyls. This development will extend the opportunities for characterizing surfaces of other silica, silica-alumina and zeolite materials,[43-46] through ubiquitous and abundant oxygens, while minimizing the need for expensive isotopic enrichment. Other applications may include studies of quantum materials, e.g., coordination of phosphine capping agents on CdSe nanoparticles via ^{31}P{^{17}O} or ^{113}Cd{^{17}O} *D*-HMQC.[47]

Acknowledgements

We would like to thank Dr. I. I. Slowing, Dr. J. Stebbins, and SASOL Ltd. for kindly providing the samples of MCM-41 silica, ^{17}O-enriched silica gel, and silica-alumina samples, respectively. This research was supported by the U.S. Department of Energy (DOE), Office of Science, Basic Energy Sciences, Materials Science and Engineering Division. The Ames Laboratory is operated for the DOE by Iowa State University under contract No. DE-AC02-07CH11358.

Keywords: DNP Solid-state NMR • indirect detection of ^{17}O through ^{29}Si • natural abundance

References:

[1] L. Lumata, A. K. Jindal, M. E. Merritt, C. R. Malloy, A. D. Sherry, Z. Kovacs, *J. Am. Chem. Soc.* **2011**, *133*, 8673-8680.

[2] A. J. Rossini, A. Zagdoun, M. Lelli, J. Canivet, S. Aguado, O. Ouari, P. Tordo, M. Rosay, W. E. Maas, C. Coperet, D. Farrusseng, L. Emsley, A. Lesage, *Angew. Chem. Int. Ed.* **2012**, *51*, 123-127.

[3] A. Zagdoun, G. Casano, O. Ouari, G. Lapadula, A. J. Rossini, M. Lelli, M. Baffert, D. Gajan, L. Veyre, W. E. Maas, M. Rosay, R. T. Weber, C. Thieuleux, C. Coperet, A. Lesage, P. Tordo, L. Emsley, *J. Am. Chem. Soc.* **2012**, *134*, 2284-2291.

[4] F. Blanc, L. Sperrin, D. A. Jefferson, S. Pawsey, M. Rosay, C. P. Grey, *J. Am. Chem. Soc.* **2013**, *135*, 2975-2978.

[5] F. Blanc, L. Sperrin, D. Lee, R. Dervisoglu, Y. Yamazaki, S. M. Haile, G. De Paepe, C. P. Grey, *J. Phys. Chem. Lett.* **2014**, *5*, 2431-2436.

[6] Z. Guo, T. Kobayashi, L.-L. Wang, T. W. Goh, C. Xiao, M. A. Caporini, M. Rosay, D. D. Johnson, M. Pruski, W. Huang, *Chem. Eur. J.* **2014**, *20*, 16308-16313.

[7] T. Kobayashi, S. Gupta, M. A. Caporini, V. K. Pecharsky, M. Pruski, *J. Phys. Chem. C* **2014**, *118*, 19548-19555.

[8] T. Gutmann, J. Liu, N. Rothermel, Y. Xu, E. Jaumann, M. Werner, H. Breitzke, S. T. Sigurdsson, G. Buntkowsky, *Chem. Eur. J.* **2015**, *21*, 3798-3805.

[9] F. A. Perras, T. Kobayashi, M. Pruski, *J. Am. Chem. Soc.* **2015**, *137*, 8336-8339.

[10] A. S. L. Thankamony, C. Lion, F. Pourpoint, B. Singh, A. J. P. Linde, D. Carnevale, G. Bodenhausen, H. Vezin, O. Lafon, V. Polshettiwar, *Angew. Chem. Int. Ed.* **2015**, *54*, 2190-2193.

[11] D. Lee, C. Leroy, C. Crevant, L. Bonhomme-Coury, F. Babonneau, D. Laurencin, C. Bonhomme, G. De Paepe, *Nat. Commun.* **2017**, *8*, 14104.

[12] N. J. Brownbill, D. Gajan, A. Lesage, L. Emsley, F. Blanc, *Chem. Commun.* **2017**, *53*, 2563-2566.

[13] T. Wolf, S. Kumar, H. Singh, T. Chakrabarty, F. Aussenac, A. I. Frenkel, D. T. Major, M. Leskes, *J. Am. Chem. Soc.* **2019**, *141*, 451-462.

[14] Z. Wang, M. P. Hanrahan, T. Kobayashi, F. A. Perras, Y. Chen, F. Engelke, C. Reiter, A. Purea, A. J. Rossini, M. Pruski, *Solid State Nuclear Magnetic Resonance* **2020**, *109*, 101685.

[15] D. Jardon-Alvarez, G. Reuveni, A. Harchol, M. Leskes, *J. Phys. Chem. Lett.* **2020**, *11*, 5439-5445.

[16] F. A. Perras, T. Kobayashi, M. Pruski, *emagres* **2018**, *7*, 35-50.

[17] A. J. Rossini, *J. Phys. Chem. Lett.* **2018**, *9*, 5150-5159.

[18] F. A. Perras, U. Chaudhary, Slowing, II, M. Pruski, *J. Phys. Chem. C* **2016**, *120*, 11535-11544.

[19] F. A. Perras, Z. R. Wang, P. Naik, Slowing, II, M. Pruski, *Angew. Chem. Int. Ed.* **2017**, *56*, 9165-9169.

[20] J. Camacho-Bunquin, M. Ferrandon, H. Sohn, D. L. Yang, C. Liu, P. A. Ignacio-de Leon, F. A. Perras, M. Pruski, P.

Accepted Manuscript

This article is protected by copyright. All rights reserved.

C. Stair, M. Delferro, *J. Am. Chem. Soc.* **2018**, *140*, 3940-3951.

[21] H. Nagashima, J. Trebosc, Y. Kon, K. Sato, O. Lafon, J. P. Amoureux, *J. Am. Chem. Soc.* **2020**, *142*, 10659-10672.

[22] V. K. Michaelis, B. Corzilius, A. A. Smith, R. G. Griffin, *J. Phys. Chem. B* **2013**, *117*, 14894-14906.

[23] M. A. Hope, D. M. Halat, P. C. M. M. Magusin, S. Paul, L. Peng, C. P. Grey, *Chem. Commun.* **2017**, *53*, 2142-2145.

[24] D. Wisser, G. Karthikeyan, A. Lund, G. Casano, H. Karoui, M. Yulikov, G. Menzildjian, A. C. Pinon, A. Purea, F. Engelke, S. R. Chaudhari, D. Kubicki, A. J. Rossini, I. B. Moroz, D. Gajan, C. Copere, G. Jeschke, M. Lelli, L. Emsley, A. Lesage, O. Ouari, *J. Am. Chem. Soc.* **2018**, *140*, 13340-13349.

[25] G. Tricot, J. Trebosc, F. Pourpoint, R. Gauvin, L. Delevoye, in *Annual Reports on Nmr Spectroscopy, Vol 81, Vol. 81* (Ed.: G. A. Webb), **2014**, pp. 145-184.

[26] A. J. Rossini, M. P. Hanrahan, M. Thuo, *Phys. Chem. Chem. Phys.* **2016**, *18*, 25284-25295.

[27] A. Brinkmann, A. P. M. Kentgens, *J. Am. Chem. Soc.* **2006**, *128*, 14758-14759.

[28] R. Q. Fu, S. A. Smith, G. Bodenhausen, *Chem. Phys. Lett.* **1997**, *272*, 361-369.

[29] Y. Ishii, R. Tycko, *J. Magn. Reson.* **2000**, *142*, 199-204.

[30] T. Kobayashi, Y. Nishiyama, M. Pruski, in *Modern Methods in Solid-state NMR: A Practitioner's Guide* (Ed.: P. Hodgkinson), The Royal Society of Chemistry, Cambridge, **2018**, pp. 1-38.

[31] J. Trebosc, J. W. Wiench, S. Huh, V. S. Y. Lin, M. Pruski, *J. Am. Chem. Soc.* **2005**, *127*, 7587-7593.

[32] N. M. Trease, T. M. Clark, P. J. Grandinetti, J. F. Stebbins, S. Sen, *J. Chem. Phys.* **2017**, *146*.

[33] T. M. Clark, P. J. Grandinetti, P. Florian, J. F. Stebbins, *Phys. Rev. B* **2004**, *70*, 064202.

[34] A. Zagdoun, G. Casano, O. Ouari, M. Schwaerzwalder, A. J. Rossini, F. Aussenac, M. Yulikov, G. Jeschke, C. Coperet, A. Lesage, P. Tordo, L. Emsley, *J. Am. Chem. Soc.* **2013**, *135*, 12790-12797.

[35] M. McMillan, J. S. Brinen, J. D. Carruthers, G. L. Haller, *Colloid Surf.* **1989**, *38*, 133-148.

[36] N. Katada, M. Niwa, *Res. Chem. Intermediates* **1998**, *24*, 481-494.

[37] A. E. Geissberger, P. J. Bray, *J. Non-Cryst. Solids* **1983**, *54*, 121-137.

[38] S. L. Carnahan, B. J. Lampkin, P. Naik, M. P. Hanrahan, Slowing, II, B. VanVeller, G. Wu, A. J. Rossini, *J. Am. Chem. Soc.* **2019**, *141*, 441-450.

[39] T. H. Walter, E. Oldfield, *J. Phys. Chem.* **1989**, *93*, 6744-6751.

[40] L. M. Peng, Y. Liu, N. J. Kim, J. E. Readman, C. P. Grey, *Nat. Mater.* **2005**, *4*, 216-219.

[41] T. Kobayashi, J. A. DiVerdi, G. E. Maciel, *J. Phys. Chem. C* **2008**, *112*, 4315-4326.

[42] X. Y. Xue, M. Kanzaki, *J. Phys. Chem. B* **2001**, *105*, 3422-3434.

[43] M. Valla, A. J. Rossini, M. Caillot, C. Chizallet, P. Raybaud, M. Digne, A. Chaumonnot, A. Lesage, L. Emsley, J. A. van Bokhoven, C. Coperet, *J. Am. Chem. Soc.* **2015**, *137*, 10710-10719.

[44] Z. J. Berkson, R. J. Messinger, K. Na, Y. Seo, R. Ryoo, B. F. Chmelka, *Angew. Chem. Int. Ed.* **2017**, *56*, 5164-5169.

[45] S. Smeets, Z. J. Berkson, D. Xie, S. I. Zones, W. Wan, X. Zou, M.-F. Hsieh, B. F. Chmelka, L. B. McCusker, C. Baerlocher, *J. Am. Chem. Soc.* **2017**, *139*, 16803-16812.

[46] A. D. Chowdhury, I. Yarulina, E. Abou-Hamad, A. Gurinov, J. Gascon, *Chem. Sci.* **2019**, *10*, 8946-8954.

[47] A. Heuer-Jungemann, N. Feliu, I. Bakaimi, M. Hamaly, A. Alkilany, I. Chakraborty, A. Masood, M. F. Casula, A. Kostopoulou, E. Oh, K. Susumu, M. H. Stewart, I. L. Medintz, E. Stratakis, W. J. Parak, A. G. Kanaras, *Chem. Rev.* **2019**, *119*, 4819-4880.

Accepted Manuscript

This article is protected by copyright. All rights reserved.

WILEY-VCH

COMMUNICATION

Entry for the Table of Contents

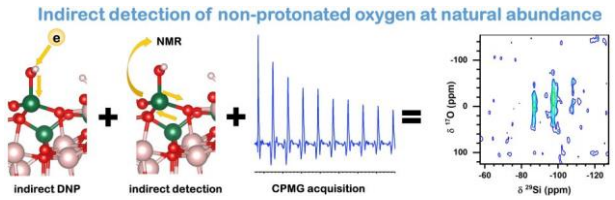

Combination of indirect DNP, indirect detection through ^{29}Si, and ^{29}Si-CPMG acquisition enabled measurements of non-protonated oxygen at natural abundance.

Key Words: NMR spectroscopy, Oxygen, Surface analysis

WILEY-VCH
Accepted Manuscript

This article is protected by copyright. All rights reserved.